Ground Motion from the August 17, 2015, Moment Magnitude 4.6 Earthquake Induced by Hydraulic Fracturing in Northeastern British Columbia

A. Babaie Mahani, Geoscience BC, Vancouver, BC, ali.mahani@mahangeo.com

H. Kao, Natural Resources Canada, Geological Survey of Canada-Pacific, Sidney, BC

J. Johnson, BC Oil and Gas Commission, Victoria, BC

C.J. Salas, Geoscience BC, Vancouver, BC

Babaie Mahani, A., Kao, H., Johnson, J. and Salas, C.J. (2017): Ground motion from the August 17, 2015, moment magnitude 4.6 earthquake induced by hydraulic fracturing in northeastern British Columbia; *in* Geoscience BC Summary of Activities 2016, Geoscience BC, Report 2017-1, p. 9–14.

Introduction

Analysis of earthquake ground motion from data recorded by regional and local seismograph networks is essential in understanding the potential seismic hazard in a region. Ground motion prediction equations (GMPE) are routinely developed and modified as more data become available, then they are used to update the available seismic hazard maps and building codes. However, the majority of the available GMPE lack data resolution at distances close to the source of the earthquakes. This lack of resolution is especially important with regard to the ground motion from larger, shallow, fluid-injection–induced events, which has the potential to damage the structures around the injection point (Novakovic and Atkinson, 2015).

Earthquakes caused by fluid injection are now common in central and eastern US (Keranen et al., 2014; Skoumal et al., 2015) and western Canada in the provinces of Alberta and British Columbia (Atkinson et al., 2016; Babaie Mahani et al., 2016). Although damage from these induced earthquakes has been observed after the larger magnitude events, such as the moment magnitude (M_w) 5.7 earthquake in November 2011 in Prague, Oklahoma (Keranen et al., 2013), smaller events in western Canada with magnitudes of 4 and higher (Atkinson et al., 2015; Eaton and Babaie Mahani, 2015; Babaie Mahani et al., in press) also require special attention due to the shallow depth of these events.

On August 17, 2015, an M_w 4.6 event occurred in the northern Montney play of British Columbia (BC), in an area where intensive hydraulic fracturing and long-term injection of gas and wastewater have taken place for decades (Babaie Mahani et al., in press). The regional seismographic stations operated by Natural Resources Canada (NRCan) in the area are too sparse to provide ground motion data at close distances. However, a local seismograph network owned by Progress Energy Canada Ltd. (Progress Energy) provided a unique dataset ranging in distance from 5 to 100 km (Figure 1a). Waveforms from this event, however, were clipped at epicentral distances as far as ~40 km, therefore, direct observation of maximum ground motion amplitudes is not possible. In this paper, ground motion amplitudes from the M_w 4.6 event at the clipped stations are estimated using the unclipped waveforms from an aftershock (M_w 3.0), which happened approximately three hours after the main shock.

Keywords: *British Columbia, induced seismicity, ground motion*

This publication is also available, free of charge, as colour digital files in Adobe Acrobat® PDF format from the Geoscience BC website: http://www.geosciencebc.com/s/DataReleases.asp.

Database

In this study, the availability of data from the Progress Energy three-component broadband sensors (Figure 1a), situated close to the hydraulic fracturing operations, provided an excellent opportunity to investigate the level of ground motion at close distances caused by induced events. Figure 1b shows seismicity and injection activity during the months of August and September 2015. Earthquakes are well clustered around the hydraulic fracturing wells. Babaie Mahani et al. (in press) studied seismic activity and fluid injection in this region from October 2014 to the end of 2015. It was found that events are better correlated in space and time with hydraulic fracturing than other types of fluid injection in the area. Events occurred at shallow depths (<2.5 km) on northwest-trending thrust faults, based on results from double difference relocation and moment tensor inversion (Babaie Mahani et al., in press).

Figure 2 shows sample raw waveforms (horizontal east-west component) from the three largest events in August and September 2015. For the August 17, M_w 4.6 event, waveform amplitudes were clipped at distances as far as ~40 km from the epicentre whereas waveform clipping was observed only at the closest station for the September 2, M_w 3.2 event (epicentral distance 7.5 km). None of the waveforms from the M_w 3.0 event on August 17 were

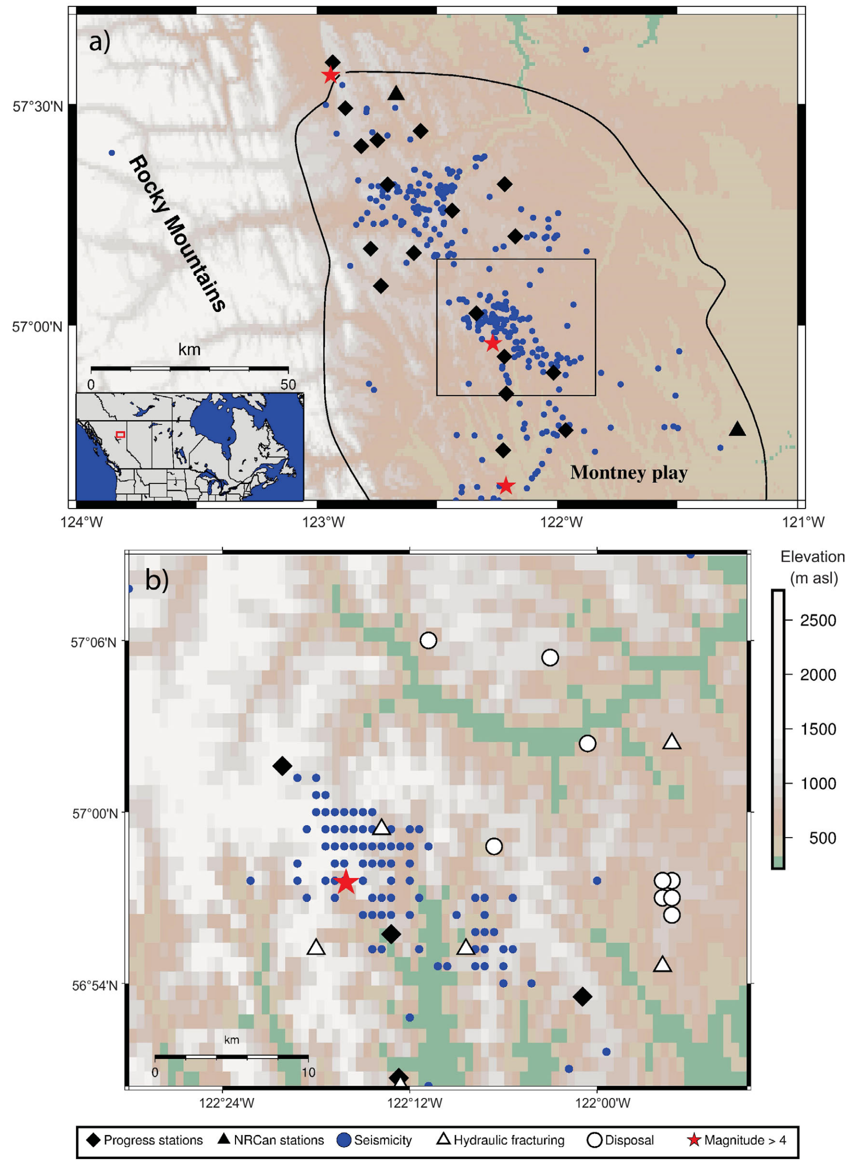

Figure 1. a) Seismic activity from 1985 to 2016 in the northern Montney play of British Columbia from Natural Resources Canada (NRCan) earthquake catalogue (Natural Resources Canada, 2016). The inset shows the region in North America. Boundary of the Montney shale gas play is shown with a black outline. The black box is the area shown in 1b. **b)** Seismic activity during the months of August and September 2015 from the Progress Energy Canada Ltd. (Progress) earthquake catalogue. The location of all wastewater disposal and gas injection wells that have been active in this area in the past five years are shown (circles). Hydraulic fracturing is shown for the months of August and September only (triangles). The star is the location of the moment magnitude (M_W) 4.6 event on August 17, 2015. Background image from Linquist et al. (2004).

clipped. Acceleration time series were obtained from the unclipped waveforms by removing the instrument response and filtering the waveforms using a second-order Butterworth bandpass filter with corner frequencies of 0.5 and 12 hertz (Hz). Figure 3 shows the three-component peak ground acceleration (PGA) versus epicentral distance for the events shown in Figure 2. In Figure 3, only values from the unclipped waveforms are shown.

Ground Motion Amplitude from the M_W 4.6 Event

Ground motion at close distances provides insights into the hazard potential of moderate-sized induced earthquakes (magnitudes of 4 and higher) to nearby structures. Analysis of ground motion from possibly induced earthquakes in the magnitude range of 3.8–4.4 in the Western Canada Sedi-

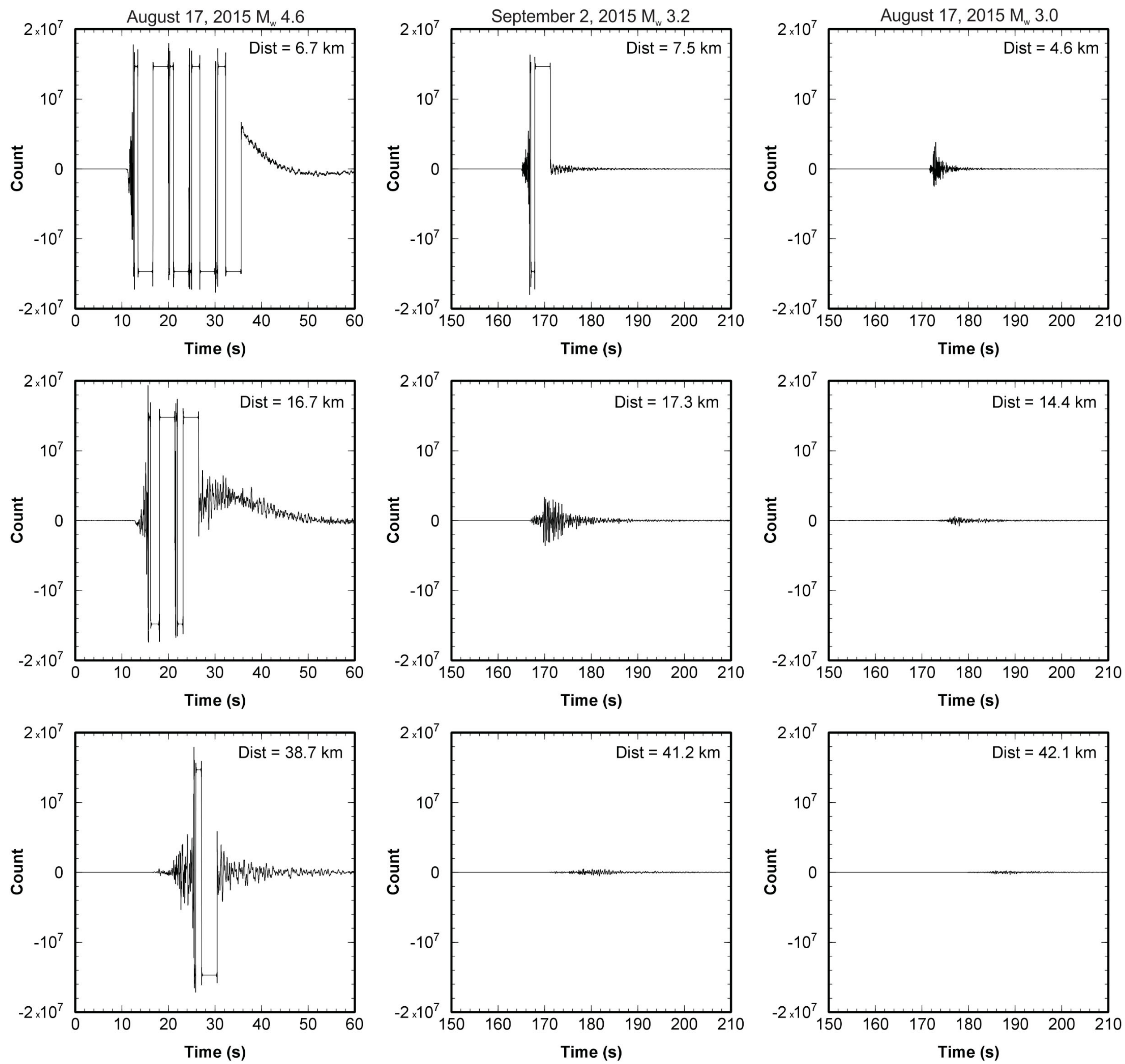

Figure 2. Sample raw seismograms (east-west component) from the three largest induced earthquakes in the months of August and September 2015. Waveforms were recorded by the broadband seismographic stations operated by Progress Energy Canada Ltd. For the August 17, moment magnitude (M_w) 4.6 event, waveform amplitudes were clipped at distances up to ~40 km. In contrast, only one station located near the September 2, M_w 3.2 event epicentre had clipped waveforms. Abbreviation: Dist, distance.

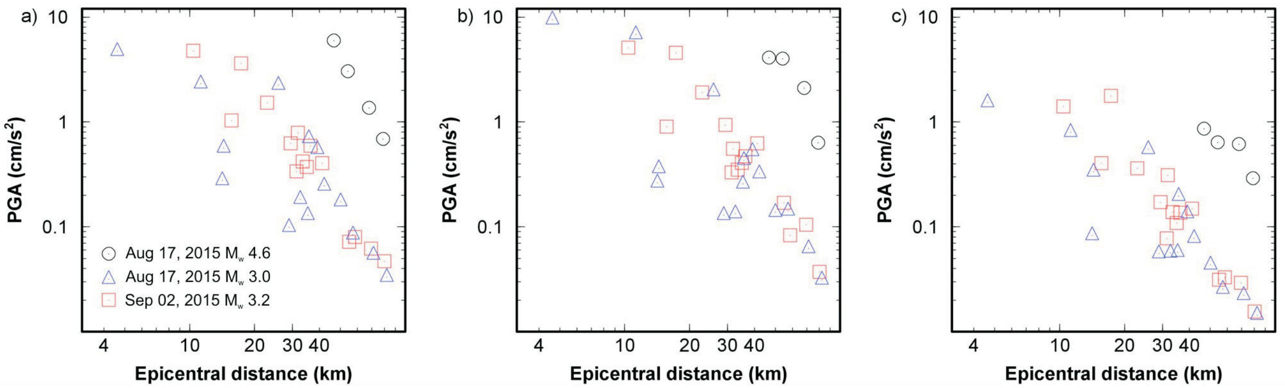

Figure 3. Three-component peak ground acceleration (PGA) versus epicentral distance for the three largest events in August and September 2015: **a)** east-west component, **b)** north-south component, and **c)** vertical component. Waveforms were recorded by the seismographic stations operated by Progress Energy Canada Ltd. Waveforms were filtered between 0.5 and 12 hertz (Hz) using a second-order Butterworth bandpass filter. Only values from unclipped waveforms are shown. Abbreviation: M_w, moment magnitude.

mentary Basin has revealed that this level of motion can be potentially damaging to nearby infrastructure due to the shallow depths of these events, although the lower stress drop as a result of shallow focal depths might limit the high frequency content of the ground motion (Atkinson, 2015; Atkinson et al., 2015). Although broadband waveform clipping as a result of instrument limitation can be common, especially at close distances (Yang and Ben-Zion, 2010), it can lead to a critical knowledge gap in characterizing the distribution of near-field ground motion when co-located strong-motion data are not available. In this case, innovative efforts should be made to derive as much ground motion information as possible from the available imperfect dataset. Here, unclipped waveforms from a smaller aftershock (August 17, 2015, M_w 3.0) that occurred approximately three hours after the M_w 4.6 event were used as a reference dataset to estimate the ground motion amplitudes for the clipped waveforms from the larger event. Both events occurred in proximity of each other with similar source and depth characteristics and were recorded by the same stations.

The total energy of a unit mass at a recording station can be related to the seismic moment, M_0, as

$$\frac{\Delta\sigma}{2\mu} M_0 = 2\rho\pi^2 \frac{A^2}{T^2} \tag{1}$$

(Lay and Wallace, 1995), where $\Delta\sigma$ is the stress drop, μ is the shear modulus, ρ is density and A is the amplitude of a wave with period T. By rearranging equation (1), a relationship can be found between the seismic moment and amplitude:

$$M_0 = 4\mu\rho\pi^2 \frac{A^2}{\Delta\sigma T^2} \tag{2}$$

Here, it is assumed that μ, ρ and $\Delta\sigma$ are similar for the two events, although, stress drop can vary from one event to another depending on depth and magnitude. With these assumptions, the ratio of seismic moments for the two events becomes

$$\frac{M_{0,4.6}}{M_{0,3.0}} = \frac{A_{4.6}^2}{A_{3.0}^2} \tag{3}$$

In equation (3), subscripts 4.6 and 3.0 refer to the M_w 4.6 and 3.0 earthquakes, respectively. The M_w 3.0 event generated a PGA value of ~10 cm/s^2 ($A_{3.0}$) at the closest distance of ~5 km on the north-south component (Figure 3b). Considering the seismic moment ratio of ~300 between the two events (i.e., $M_{0,4.6}/M_{0,3.0}$ = 300), the peak amplitude of ground acceleration generated by the M_w 4.6 event at this distance (~5 km) can be estimated to be ~173 cm/s^2 (~17% gravity [g]). Ground motion from the M_w 3.0 event at a distance of ~40 km is ~0.5 cm/s^2 on the north-south component, therefore, the equivalent ground motion at this distance for the M_w 4.6 event could be ~9 cm/s^2.

Figure 4 shows the estimated, three-component PGA values as a function of epicentral distance for the M_w 4.6 event. For distances >40 km, the estimated values can be verified by the observed ones from unclipped waveforms (triangles, Figure 4). The good match between the estimated and observed data points confirms the validity of equation (3). The felt threshold (0.3% g), damage threshold (6.2% g) and moderate damage threshold (22% g) levels shown in Figure 4 are based on Worden et al. (2012). From the observed values in Figure 4, the M_w 4.6 event could have been felt at distances as far as 60 km from the epicentre. This is consistent with the felt reports received by NRCan with some coming from far away communities, such as Charlie Lake, BC (located ~100 km to the southeast of the M_w 4.6 epicentre). Also, based on the results shown in Figure 4, the zone of potential damage could be as far as ~10 km.

The uncertainty of the estimated PGA values for the M_w 4.6 event is an important factor that deserves further investigation. For the purpose of verification, the possible level of

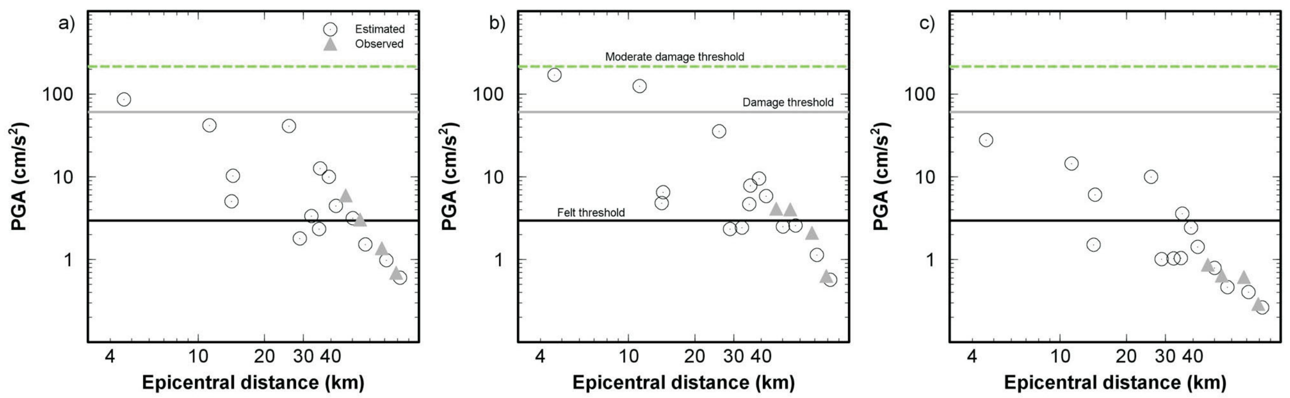

Figure 4. Estimated peak ground acceleration (PGA) for the **a)** east-west, **b)** north-south and **c)** vertical components of the August 17, 2015, moment magnitude (M_w) 4.6 event determined from the unclipped ground motion data of the smaller M_w 3.0 event using equation (3). Values as high as ~173 cm/s^2 (~17% gravity) are estimated for places close to the epicentre (~5 km or less). The three thresholds (felt, damage, moderate damage) are taken from Worden et al. (2012). The estimated PGA values are remarkably consistent with the observed ones from unclipped waveforms at distances of >40 km (shown as grey triangles).

errors when equation (3) is used for ground motion prediction is quantitatively assessed. Specifically, the M_w 3.0 event is first used to estimate the PGA values of the M_w 3.2 event on September 2, which had only one clipped waveform at the closest epicentral distance of 7.5 km (Figure 2). The estimated values for distances >7.5 km were then compared to the observed ones measured directly from the unclipped waveforms and the results are shown in Figure 5. For each data point in Figure 5, the epicentral distance for the M_w 3.0 event (which is used to obtain the estimated PGA) differs from that of the M_w 3.2 event by <5 km, thus the propagation and attenuation effects are negligible. Overall, the majority of the difference between observed and estimated PGA values is a factor of ~3. It seems that equation (3) tends to overestimate the PGA by a factor of ~2 for most data points at distances ≥40 km. In contrast, both underestimation and overestimation can happen at closer distances. Although it is difficult to determine the exact cause of this discrepancy with this limited dataset, it could be speculated that perhaps variations in local geological setting and site condition could be important factors.

Finally, Figure 6 shows the estimated and observed PGA of the geometric mean of the horizontal components from the M_w 4.6 event versus hypocentral distance (the source depth is set at 2 km). The solid line corresponds to the prediction

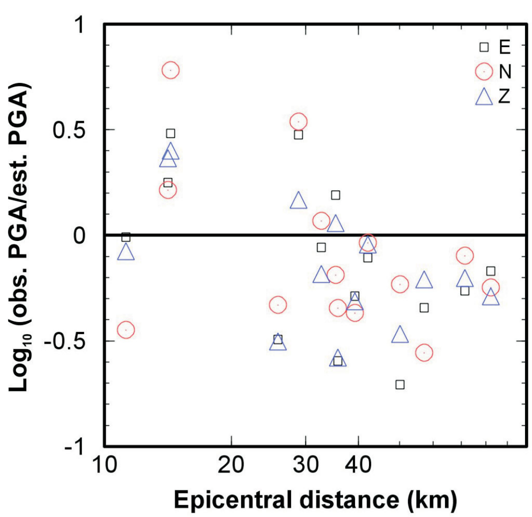

Figure 5. Plot of the ratio between the observed and estimated peak ground acceleration (PGA) of the three components for the September 2, 2015, moment magnitude (M_w) 3.2 event. Waveforms from the smaller August 17, 2015, M_w 3.0 event were used in the calculation using equation (3). Abbreviations: E, east-west component; est., estimated; N, north-south component; obs., observed; Z, vertical component.

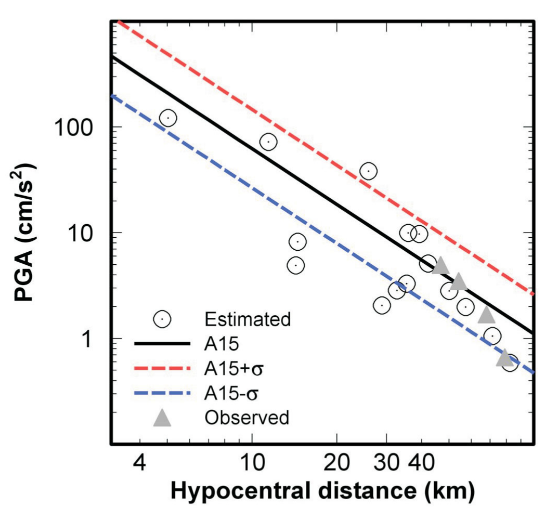

Figure 6. Estimated and observed peak ground acceleration (PGA) values of the geometric mean of the horizontal components from the M_w 4.6 event, August 17, 2015. Solid line (A15) corresponds to the prediction by the Atkinson (2015) model. Dashed lines mark the ±0.37 deviation (in logarithmic unit) from the solid line, corresponding to one standard deviation (σ) of the ground motion prediction model.

by the Atkinson (2015) model for small to moderate events at short hypocentral distances. This model is based on the Next Generation Attenuation (NGA)-West2 database (Ancheta et al., 2014) at hypocentral distances <40 km, which is suitable for applications to seismic hazard from induced earthquakes. Both the estimated and observed values appear to be in good agreement with the prediction model within its standard deviation (dashed lines, Figure 6).

Conclusion

Waveforms from the August 17, 2015, moment magnitude (M_w) 4.6 event were clipped at distances up to ~40 km from the epicentre; an indicator of large ground motion at close distances. Using the unclipped ground motion from a smaller M_w 3.0 aftershock, the authors estimate that the peak ground acceleration (PGA) from the M_w 4.6 event could have been as high as ~173 cm/s^2 (~17% gravity) at an epicentral distance of ~5 km. Although there was no reported damage from this shallow induced event, ground motion from this event could have exceeded the damage threshold of structures if it had happened in a populated area.

Acknowledgments

The authors would like to thank M. Norton with Progress Energy Canada Ltd. for providing waveform data and constructive comments on the manuscript. Financial support for this project was partially provided by the Canadian Association of Petroleum Producers and the BC Oil and Gas Research and Innovation Society.

References

Ancheta, T.D., Darragh, R.B., Stewart, J.P., Seyhan, E., Silva, W.J., Chiou, B.S.J., Wooddell, K.E., Graves, R.W., Kottke, A.R., Boore, D.M., Kishida, T. and Donahue, J.L. (2014): NGAWest2 database; Earthquake Spectra, v. 30, no. 3, p. 989–1005.

Atkinson, G.M. (2015): Ground-motion prediction equation for small-to-moderate events at short hypocentral distances, with application to induced-seismicity hazards; Bulletin of Seismological Society of America, v. 105, p. 981–992.

Atkinson, G., Assatourians, K., Cheadle, B. and Greig, W. (2015): Ground motions from three recent earthquakes in western Alberta and northeastern British Columbia and their implications for induced-seismicity hazard in eastern regions; Seismological Research Letters, v. 86, p. 1022–1031.

Atkinson, G.M., Eaton, D., Ghofrani, H., Walker, D., Cheadle, B., Schultz, R., Scherbakov, R., Tiampo, K., Gu, Y.J., Harrington, R., Liu, Y., van der Baan, M. and Kao, H. (2016): Hydraulic fracturing and seismicity in the Western Canada Sedimentary Basin; Seismological Research Letters, v. 87, p. 631–647.

Babaie Mahani, A., Kao, H., Walker, D., Johnson, J. and Salas, C. (2016): Performance evaluation of the regional seismograph network in northeast British Columbia, Canada, for monitoring of induced seismicity; Seismological Research Letters, v. 87, p. 648–660.

Babaie Mahani, A., Schultz, R., Kao, H., Walker, D., Johnson, J. and Salas, C. (in press): Fluid injection and seismic activity in the northern Montney play, British Columbia, Canada, with special reference to the 17 August 2015 M_W 4.6 induced earthquake; Bulletin of Seismological Society of America.

Eaton, D.W. and Babaie Mahani, A. (2015): Focal mechanisms of some inferred induced earthquakes in Alberta, Canada; Seismological Research Letters, v. 86, p. 1078–1085.

Keranen, K.M., Savage, H.M., Abers, G.A. and Cochran, E.S. (2013): Potentially induced earthquakes in Oklahoma, USA: links between wastewater injection and the 2011 M_W 5.7 earthquake sequence; Geology, v. 41, p. 699–702.

Keranen, K.M., Weingarten, M., Abers, G.A., Bekins, B.A. and Ge, S. (2014): Sharp increase in central Oklahoma seismicity since 2008 induced by massive wastewater injection; Science, v. 345, p. 448–451.

Lay, T. and Wallace, T.C. (1995): Modern Global Seismology; Academic Press, San Diego, California, 522 p.

Lindquist, K.G., Engle, K., Stahlke, D. and Price, E. (2004): Global topography and bathymetry grid improves research efforts; Eos, Transactions, American Geophysical Union, v. 85, no. 19, p. 186, URL <http://onlinelibrary.wiley.com/doi/10.1029/2004EO190003/full> [November 2016].

Natural Resources Canada (2016): Earthquakes Canada; Natural Resources Canada, URL <http://earthquakescanada.nrcan.gc.ca> [November 2016].

Novakovic, M. and Atkinson, G.M. (2015): Preliminary evaluation of ground motions from earthquakes in Alberta; Seismological Research Letters, v. 86, p. 1086–1095.

Skoumal, R.J., Brudzinski, M.R. and Currie, B.S. (2015): Earthquakes induced by hydraulic fracturing in Poland Township, Ohio; Bulletin of Seismological Society of America, v. 105, p. 189–197.

Worden, C.B., Gerstenberger, M.C., Rhoades, D.A. and Wald, D.J. (2012): Probabilistic relationships between ground-motion parameters and modified Mercalli intensity in California; Bulletin of Seismological Society of America, v. 102, p. 204–221.

Yang, W. and Ben-Zion, Y. (2010): An algorithm for detecting clipped waveforms and suggested correction procedures; Seismological Research Letters, v. 81, p. 53–62.